

# Michaelis-Menten dynamics of a polymer chain out of a dichotomous ATP-based motor

Alessandro Fiasconaro<sup>1,2</sup>, Juan José Mazo<sup>1,2</sup>, Fernando Falo<sup>1,3</sup>

<sup>1</sup> Departamento de Física de la Materia Condensada, Universidad de Zaragoza, C/ Pedro Cerbuna, 12 50009 Zaragoza, Spain

<sup>2</sup> Instituto de Ciencia de Materiales de Aragón, CSIC-Universidad de Zaragoza, C/ Pedro Cerbuna, 12 50009 Zaragoza, Spain

<sup>3</sup> Instituto de Biocomputación y Física de Sistemas Complejos, Universidad de Zaragoza, C/ Pedro Cerbuna, 12 50009 Zaragoza, Spain

E-mail: [afiascon@unizar.es](mailto:afiascon@unizar.es)

**Abstract.** We present a model of an ATP-fueled molecular machine which push a polymer through a pore channel. The machine acts between two levels (working-waiting), and the working one remains active for a fixed time giving a constant force. The machine activation rate can be put in relationship with the available ATP concentration in the solution, which gives the necessary energy supply. The translocation time shows a monotonic behaviour as a function of the activation frequency and the velocity follows a Michaelis-Menten law that arises naturally in this description. The estimation of the stall force of the motor follows a corrected Michaelis-Menten law which still is to be checked in experimental investigation. The results presented agree with recent biological experimental findings.

## 1. Introduction

In the last years there has been an important progress in the experimental and theoretical study of transport mechanisms of molecules inside cells and/or through cell membranes [1]. This effort is attracting nowadays more and more attention from researchers in different scientific disciplines. The increasing interest in this subject is related to the intrinsic importance of understanding the basic mechanisms of the living systems, but also to the enormous improvement of technological capabilities at nanometer length scale. These, on the one hand, allow to detect and to measure mechanisms at the nanoscale, and, on the other hand, open the possibility of constructing from scratch structures (with both natural and synthetic materials) able to imitate the biological functioning [2]. In this context, the passage of biomolecules through nanopores is ubiquitous, both in biological and nanotechnological processes. Examples of these two types are the passage of mRNA through nuclear pores [3] or the translocation of DNA in graphene pores [4].

In most cases, translocation is driven by constant fields in the pore or by the difference in chemical potential between the two sides of the membrane. However, in

some cases the translocation is assisted by an ATP-based molecular motor [5]. This is the case of DNA bacteriophages in which the incoming DNA has to overcome a huge pressure inside the virus capsid. This makes this kind of motors, possibly, the most powerful of those known. In this type of motors ATP hydrolysis is the fuel of the process.

In this paper we model the translocation process of a 1d chain pushed by a molecular motor activated by ATP absorption. The motor is able to drive with a constant force a polymer chain in one direction, while in its activated state. The polymer diffuses freely otherwise [6, 7]. The work reveals the Michaelis-Menten (MM) behaviour of the polymer velocity and relates it with the MM enzymatic reaction, according to a microscopic re-interpretation of the MM kinetics which is a very actual topic of investigation [8, 9, 10].

We will also study the behaviour of the motor against a pulling force, the motor stall force, and its ability to package the polymer in a finite region, as a first approach to a capsid effect.

The aim of this work is to present a simple model which captures the main physical ingredients of the process. Remarkably, the model is able to well describe some experimentally observed results and make new predictions. The model could be also applied to different kinds of systems. In this spirit, we do not pretend here to give a detailed description of a particular molecular motor.

## 2. The model

The polymer is modeled as a 1-dimensional chain of  $N$  dimensionless monomers connected by harmonic springs [11]. The total potential energy is  $V_{\text{har}} = \frac{k}{2} \sum_{i=1}^{N-1} (x_{i+1} - x_i - d_0)^2$ , where  $k$  is the elastic constant,  $x_i$  the position of the  $i$ -th particle, and  $d_0$  the equilibrium distance between adjacent monomers. Along the work  $d_0 = 1$  and  $k = 1$ .

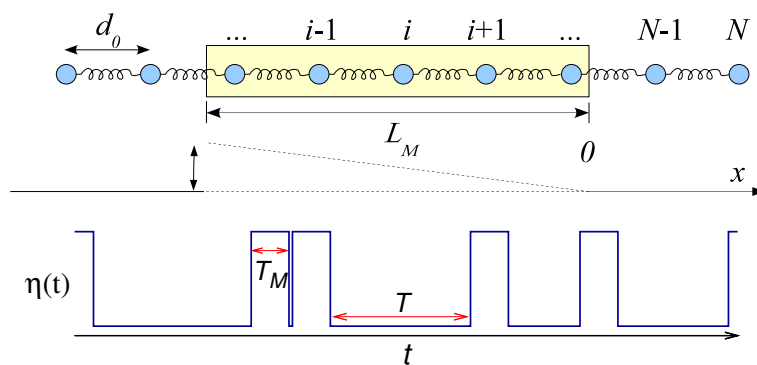


**Figure 1.** Scheme of the dichotomous pushing force acting on a polymer chain compound by  $N$  monomers.  $T_M$  is the working time of the motor, supposed fixed.  $T$  is the mean waiting time in the inactive state. The motor acts on a region of length  $L_M$ , where the motor action can be expressed by the linear potential  $-\eta(t)F_M x$  (with  $\eta = 1$  for the active state and  $\eta = 0$  for the inactive one), indicated in the middle figure by two dotted lines.

The translocation is helped by the presence of an ATP activated molecular motor. It has spatial width  $L_M$  and we set at  $x = 0$  its right edge (see figure 1). The motor is characterized by a fixed working time  $T_M$  which follows the ATP absorption, which, in its turn, occurs after a mean waiting time  $T$ , depending on the very ATP concentration. In this sense the ATP molecules act on the motor as a shot noise contribution able to switch on its activity. The motor exerts a dichotomous force  $F_M\eta(t)$  on the particles inside the motor ( $x \in [-L_M, 0]$ ), where  $\eta(t)$  is 1 during the working time and 0 otherwise. As shown in [12], the ATP absorption follows an exponential distribution of waiting times: the probability for an ATP adsorption in a time between  $t'$  and  $t'+dt'$  after the last activity is proportional to  $e^{-t'/T}$ . Thus, the activation probability of the motor is given by  $P_{\nu} = 1 - e^{-t'/T}$  with  $t'$  the motor residence time in its inactive state.

The dynamics of the  $i^{\text{th}}$  monomer of the chain is described by the following overdamped Langevin equation:

$$\dot{x}_i = -V'_{har} + F_M\eta_i(t) + \xi_i(t), \quad (1)$$

where the damping (considered the same for all the monomers, which feel the viscosity independently on each other) is included in the normalized time. In the above dimensionless equation  $d_0$  is taken as the unit of length, the force is expressed in units of  $kd_0$ , and the energy in units of  $kd_0^2$ .  $\xi_i(t)$  are the Gaussian uncorrelated thermal fluctuations which follow the usual statistical properties  $\langle \xi_i(t) \rangle = 0$  and  $\langle \xi_i(t)\xi_j(t+\tau) \rangle = 2D\delta_{ij}\delta(\tau)$  with  $(i, j = 1\dots N)$ .

### 3. Energy supply

The energy used by the motor to provide the driving is given by the ATP hydrolysis. In our model, each ATP hydrolysis just activates the motor for a fixed working time  $T_M$ . This description avoids more complex details which are beyond the spirit of our work.

As a consequence of the ATP absorption, the motor changes its conformational state and exerts a mean force  $F_M$  during a fixed time  $T_M = 1/\nu_0$ . After that time the motor returns to its inactive state. A new force is applied when the next ATP suitable quantity is absorbed. It happens after a mean time  $T = 1/\nu$ , which follows an exponential distribution of waiting times. That way in our description the activation frequency is proportional to the ATP concentration [13]:  $\nu \propto [ATP]$ . The hypothesis that the motor works for a fixed time and that the statistics of the arrival of the ATP molecules happens in an exponential distribution appears realistic in good approximation as put in evidence by different experimental works [9, 10, 12, 14, 15].

With this definition the Michaelis-Menten law arises naturally from the model. The motor duty ratio, the fraction of time that it is active, is given by

$$\frac{T_M}{T_M + T} = \frac{\nu}{\nu_0 + \nu} = \frac{[ATP]}{k_M + [ATP]}, \quad (2)$$

which is a Michaelis-Menten law. The only hypothesis included in the derivation of the last equality is that the motor activation rate  $\nu$  is proportional to the ATP concentration, being  $k_M = [ATP]\nu_0/\nu$  the Michaelis constant.

The relationship between the mechanical description presented and the Michaelis-Menten law is deeper than only the statistical ansatz  $\nu \propto [ATP]$ . In the Michaelis-Menten enzymatic reaction,



the rate  $k_1$  represents the probability to form the compound  $Z$  per unit of time and per unit of  $S$  ( $[ATP]$ ), and  $k_2$  gives the probability to form the product  $P$  per unit of time. In our mechanical and individual case (single motor and single ATP event)  $Z$  represents the ATP bound to the motor, which occurs with the frequency  $\nu$  ( $\sim k_1[ATP]$ ), while  $P$  represents the motor action, which is completed within a time  $T_M = 1/\nu_0$  ( $\nu_0 \sim k_2$ ). These relationships are in agreement with the definition of the Michaelis constant  $k_M = k_2/k_1$ .

#### 4. Results

We have numerically solved the Langevin equation (1). We are mainly interested in the behaviour of the translocation time  $\tau$  and velocity  $v$  as a function of the motor activation frequency  $\nu$ . We will compare our results to some theoretical predictions, derived below. For every computed point we performed at least  $N_{exp} = 10,000$  numerical experiments (for low frequency up to 50,000) using a stochastic Runge-Kutta algorithm with a time step  $dt = 0.01$ . The polymer is compound by  $N$  monomers and starts with all the spring at the rest length and the last monomer of the chain at  $x_N = 0$ , just at the exit of the motor. The noise intensity is held fixed at the value  $D = 0.01$  and the intensity of the force is  $F_M = 0.1$ . We have chosen  $L_M/d_0 = 5.5$ .

*Polymer translocation.* We start studying the mean translocation time and velocity of the polymer driven by the motor. With respect to the polymer velocity, by summing up the  $N$  terms of equation (1) and averaging in time, we obtain for the centre of mass of the chain the mean velocity  $v$ :

$$v = \frac{F_M}{N} \sum_{i=1}^N \langle \eta_i(t) \rangle = \frac{F_M}{N} \frac{n_{\text{mot}}^{\text{on}}(\nu)}{1 + \nu_0/\nu}. \quad (4)$$

Here  $n_{\text{mot}}^{\text{on}}(\nu)$  is the mean number of monomers inside the motor during its activity, a number which is expected to depend weakly on  $\nu$ . Thus, the mean velocity of the polymer depends on the force felt by the  $n_{\text{mot}}^{\text{on}}$  monomers inside the machine which operates for fraction of time  $\nu/(\nu_0 + \nu)$ , and the polymer shows a Michaelis-Menten law for the velocity weakly moderated by the function  $n_{\text{mot}}^{\text{on}}(\nu)$ . Note that this velocity goes to zero as  $1/N$  for a large chain as expected for a motor which acts on a small number of monomers and a polymer which moves in a dissipative media.

We also want to mention that equation (4) it is also valid in other interesting situations too. For instance, systems with random distributions of  $T_M$  values with small dispersion around its mean value or the case of a minimum threshold time for the motor activation, which effectively imposes a maximum cutoff frequency in the system (in this case  $1/\nu = T_{\text{thres}} + T$ ).

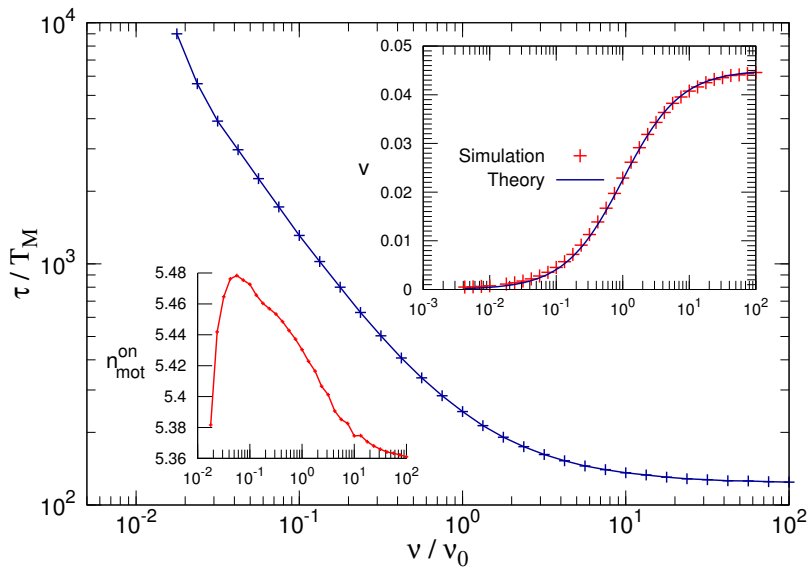


**Figure 2.** Log-Log plot of the mean first passage time  $\tau$  as a function of the mean frequency of the fluctuating force. Upper inset: mean velocity, following the Michaelis-Menten law given by equation (5). Bottom inset: mean number of particle inside the motor during its active state. The thermal noise intensity is  $D = 0.01$  and  $k = 1$ .

Figure 2 shows the main observables of the system and their frequency dependence. The translocation time  $\tau$  is computed as the mean first passage time (MFPT), i.e. the average over the  $N_{exp}$  realizations of the time spent by the centre of mass of the chain to reach the position  $x = 0$ . It is observed that this time decreases monotonously as  $\nu$  increases and reaches a limit value for large enough values of  $\nu$  ( $T$  goes to zero and the motor is ‘on’ most of the time). The relation between translocation velocity  $v$  and time  $\tau$  is not trivial at all, as can be seen in [16] and [17].

The physics of the problem is regulated by the mean number of monomers in the motor during the working time,  $n_{mot}^{on}$ , a number directly related with the elasticity of the chain. As seen in the inset, for the used parameters this number is close to  $L_M/d_0$  and does not change importantly in all the frequency range covered. Thus, as predicted by equation (4) the polymer velocity follows a Michaelis-Menten law (see inset in figure 2):

$$v \simeq v_{HR}^0 / (1 + \nu_0/\nu) \quad (5)$$

with  $v_{HR}^0$  the high frequency limit ( $v_{HR}^0 = 0.0450$  in the plotted case, which is close to  $0.0458 = F_M n_M / N$  with  $F_M = 0.1$ ,  $N = 12$  and  $n_M = L_M/d_0 = 5.5$ ). Equation (5) allows for a direct experimental fit once the velocity at high ATP concentration (the high rate limit of our system) is measured. With respect to the low frequency limit, we can see from the equation that  $v$  goes to zero as  $v \simeq v_{HR}^0 (\nu/\nu_0) \simeq (F_M n_M / N) (\nu/\nu_0)$ .

*Elastic Constant.* In order to better understand how the elasticity of the chain acts on the translocation dynamics, we have computed the mean velocity and first passage time ( $v$  and  $\tau$ ) for different values of the elastic constant between monomers  $k$  (see figure 3). We notice that similar behaviour is observed for the different values

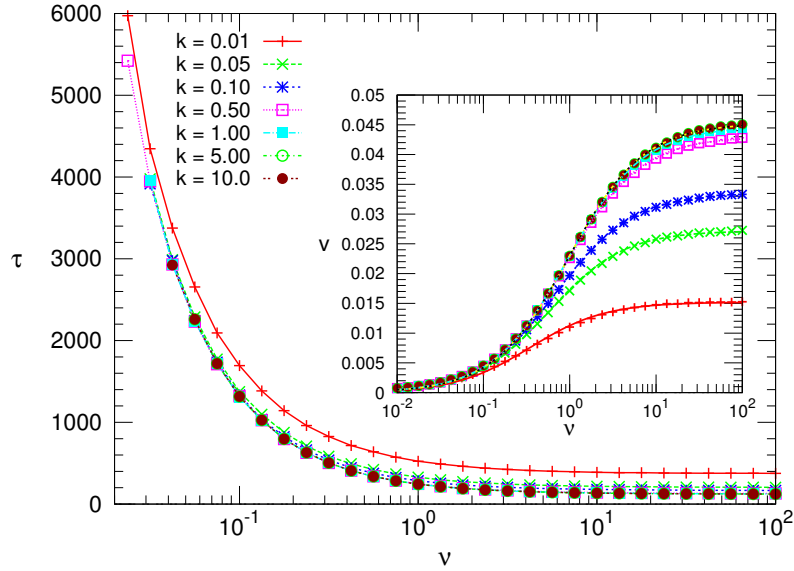


**Figure 3.** Translocation time and velocity (inset) for different values of the elasticity of the chain  $k$ . Lines in the inset show the fit to  $v = v_{HR}^0 / (1 + b\nu_0/\nu)$  where  $b = 1$  for  $k > 0.5$ .

considered. As expected, a smaller  $k$  gives a lower velocity, the polymer enlarges and the mean number of monomers in the machine diminishes. At low  $k$ ,  $n_{\text{mot}}^{\text{on}}$  changes significantly with  $\nu$  and  $v$  shows deviations with respect to the predictions of equation (5) but can be nicely fit by a slightly modified law (see caption of figure 3). For high  $k$  ( $k > 1$ ) we reach the rigid chain limit of the system.

*Translocation in the presence of a pull force.* A set of simulations has been performed by applying a pull force  $F_p$  on the left extremum of the chain, acting against the motor (see figure 4). The initial condition is set with the polymer centre of mass in the centre of the machine. The velocity of the centre of mass is measured waiting for the exit on the left or on the right of the potential region.

In this case, the mean velocity is given by

$$v = \frac{F_M}{N} \frac{n_{\text{mot}}^{\text{on}}(\nu; F_p)}{1 + \nu_0/\nu} - \frac{F_p}{N}, \quad (6)$$

where the last term  $F_p/N$  modifies equation (4) by taking into account the presence of an external force acting against the machine. There we emphasize that the presence of a pulling force also modifies the value of  $n_{\text{mot}}^{\text{on}}$  with respect to the unforced value.

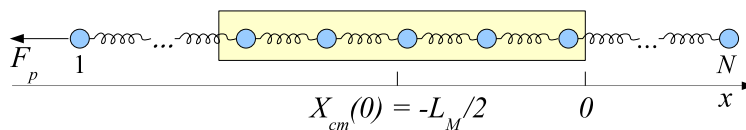


**Figure 4.** A pull force  $F_p$  is applied at the chain to measure the stall force of the motor.

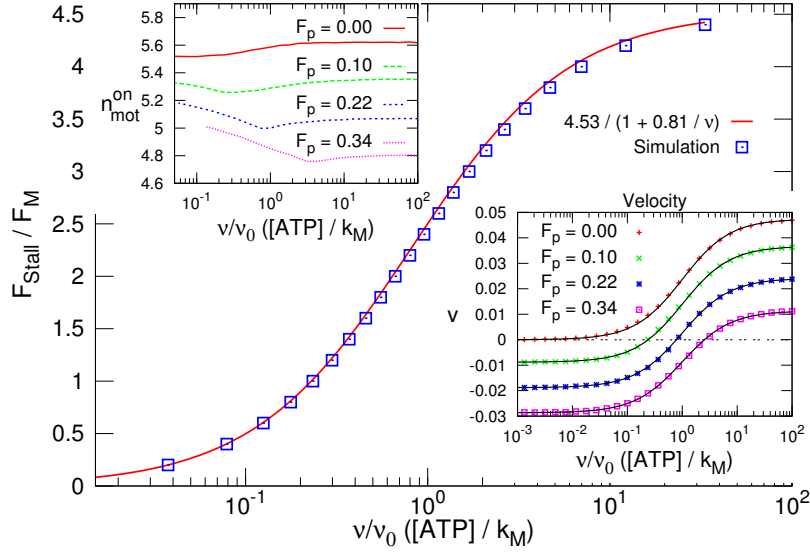


**Figure 5.** Stall force as a function of the frequency of the dichotomous driving and prediction of equation (10). The insets show, for four values of  $F_p$ ,  $n_{\text{mot}}^{\text{on}}(\nu)$  (upper inset) and the mean velocity (lower inset) computed (symbols) and predicted (lines) by equation (7).

Assuming again a weak dependence on  $\nu$  and  $F_p$  for  $n_{\text{mot}}^{\text{on}}$  we can rewrite the previous equation as

$$v \simeq \frac{v_{HR}^p}{1 + \nu_0/\nu} + \frac{v_{LR}^p}{1 + \nu/\nu_0} \quad (7)$$

where  $v_{LR}^p = -F_p/N$  is the low frequency limit of  $v$  and  $v_{HR}^p$  the high frequency one,  $v_{HR}^p = (F_M n_{\text{mot};HR}^{\text{on}} - F_p)/N$ .

Figure 5 shows (lower inset) our numerical results for the polymer velocity in the presence of a pull and it allows for a comparison against the theoretical predictions. As seen in the figure, the polymer mean velocity can be understood in terms of equation (7). Figure 5 shows the excellent agreement between this equation and the numerical calculations once the low and high ATP concentrations (low and high frequency) values are determined. The value of  $v_{HR}^p$  present in that equation can be evaluated experimentally by using the values of the velocity curves for high ATP concentrations [15]. A rough estimation can be also given by  $v_{HR}^p \simeq (F_M L_M / d_0 - F_p) / N$ .

We have also studied the frequency dependence of  $n_{\text{mot}}^{\text{on}}(\nu; F_p)$ . As visible in the top inset of figure 5, this quantity depends weakly on  $\nu$  for all the pulling forces and decreases slightly with  $F_p$  for all the frequencies. Then the velocity of the polymer shows the expected Michaelis-Menten type behaviour for all the different pull forces used in the calculations ( $F_p = 0.1, 0.22, 0.34$ ). We have verified numerically that we can consider  $n_{\text{mot}}^{\text{on}}(\nu, F_p) \simeq n_{\text{mot};HR}^{\text{on}}(F_p) \simeq n_{\text{mot};HR}^{\text{on}}(0) - aF_p$ . In our case  $a \simeq 2.35$  and  $n_{\text{mot};HR}^{\text{on}}(0) \simeq 5.59$ , obtained through a fit procedure of  $n_{\text{mot};HR}^{\text{on}}(F_p)$ , the high rate values of  $n_{\text{mot}}^{\text{on}}(\nu, F_p)$ .

*Stall Force.* We will study now the stall force  $F_{stall}$  of the system, which is the value of the pull force  $F_p$  for which the polymer velocity is zero. In formulas

$$F_{stall} = F_p(v = 0) = F_M \frac{n_{mot}^{on}(\nu, F_p)}{1 + \nu_0/\nu} \simeq F_M \frac{n_{mot;HR}^{on}(F_p)}{1 + \nu_0/\nu}. \quad (8)$$

Here we have used the weak frequency dependence of  $n_{mot}^{on}$  as suggested by the inset of figure 5. A simple approximation for  $n_{mot;HR}^{on}(F_p)$  is to assume  $n_{mot;HR}^{on} = L_M/d_0$ . As discussed above, a more realistic one is to take the linear dependence  $n_{mot;HR}^{on}(F_p) \simeq n_{mot;HR}^{on}(0) - aF_p$ . Substituting the latter expression in equation (8), we obtain

$$F_p = F_M \frac{n_{mot;HR}^{on}(0)}{1 + \nu_0/\nu} - F_M \frac{aF_p}{1 + \nu_0/\nu}. \quad (9)$$

By solving with respect to  $F_p$ , and introducing  $F_{stall}$ , we obtain

$$F_{stall} \simeq \frac{F_{stall}^{HR}}{1 + b\nu_0/\nu} \quad (10)$$

where  $b = 1/(1 + aF_M)$  and  $F_{stall}^{HR} \simeq bF_M n_{mot;HR}^{on}(0)$  is the high frequency stall force.

Figure 5 shows our numerical results for the polymer stall force problem and compares them to our theoretical predictions. We find an excellent agreement with the predictions of our equation (10), where  $b \simeq 0.81$  and  $F_{stall}^{HR} \simeq 0.453$ . These numbers results from the values of  $a \simeq 2.35$  and  $n_{mot;HR}^{on}(0) \simeq 5.59$  obtained above..

In this model, the stall force is *not weakly* dependent on the frequency  $\nu$ , but changes from 0 to  $4.5F_M$  in the range of rate variation of figure 5. Thus an experimental investigation can easily verify the stall force frequency dependence by lowering the ATP concentration in the surroundings of the motor. This way the working model can be verified and tested, and also compared with different models. ‡

*Stall force for different  $k$ .* We have made a number of simulations to study the dependence of the stall force with the elasticity constant  $k$ . The results are plotted in figure 6 where the stall force is drawn as a function of the frequency  $\nu$  for various values of  $k$ . We can observe that the stall force increases with  $k$  and shows a saturation behaviour at high  $k$  (see the curves for  $k = 5$  and  $k = 10$ ) similar to the one of the velocity (inset of figure 3).

The MM behaviour predicted by equation (10) is observed for all the curves. The inset of the figure shows the behaviour of the coefficients  $F_{stall}^{k,HR}$  and  $b$  of the equation. As expected, the rigid chain (high  $k$ ) follows an exact MM law,  $b = 1$  in equation (10).

*Polymer packing.* One of the recent most relevant activity in the field is the study of the translocation features in the DNA packing problem driven by molecular motors [12, 14, 15]. One example is the  $\phi 29$ , a bacteriophage virus which is able to inject his DNA in a bacteria in order to replicate, and then repack it in his capsid. Remarkable experiments [14] have measured the force of the motor as a function of the number

‡ We refer in particular to the outcomes of a similar motor model assisted by both a sinusoidal time dependence [16], and a pure dichotomous driving [17]. Besides the not trivial behaviours of  $F_{Stall}$  as a function of the frequency, a very weak variation of its values is there observed.



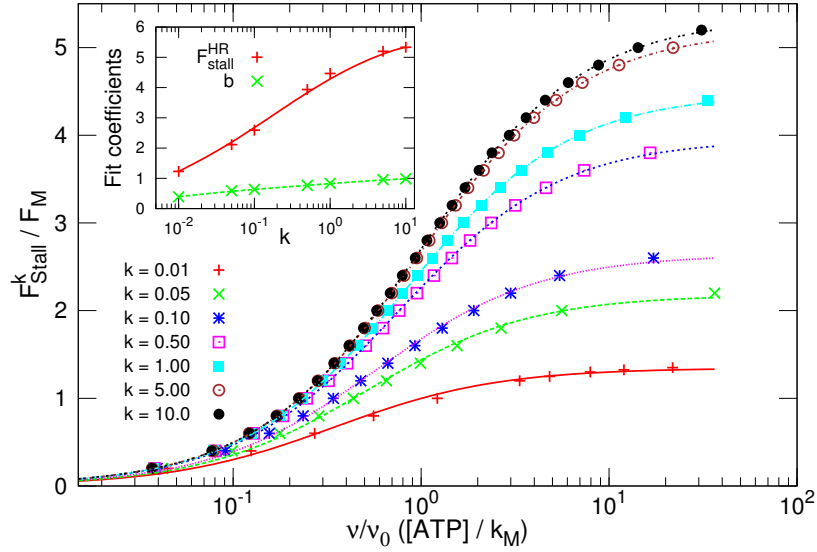


**Figure 6.** Stall force  $F_{stall}^k$  for various values of the elastic parameter  $k$ . Lines are the best fit according to equation (10) and the inset shows the values of the fit parameters for the different  $k$ .

of monomers entered in the capsid. The model here depicted is able to qualitatively reproduce the results there reported.

We performed a set of calculations where the chain is pushed into a limited portion of space. Figure 7 shows the scheme of the motor of length  $L_M$  that pushes the polymer inside a region of length  $L_{Caps}$ . The polymer starts with the last monomer on the right at the position  $x = 0$ . This particle ( $N$ -th monomer in the figure) cannot pass the wall on the right. Once there, the polymer begins to compress and the pressure on the particles inside the capsid increases more and more avoiding in some cases the completion of the translocation process. To consider excluded volume effects and maintain the relative order of the monomers, a repulsive only Lennard-Jones potential has been taken into account in the model:  $V_{LJ}(r) = 4\epsilon[(\frac{\sigma}{r})^{12} - (\frac{\sigma}{r})^6]$  for  $r \leq 2^{1/6}\sigma$ , and 0 otherwise. We used  $\epsilon = 1$ , and  $\sigma = 0.1$ .

Figure 8 plots  $F_{in}$ , the mean force acting on the last monomer entering in the capsid, as a function of the total number of monomers entered. The capsid width is  $L_{Caps}/d_0 = 8$  and the chain length is  $N = 36$  monomers. It shows that, until the size of the entered polymer approximately equals the size of the capsid, the force grows up very slowly. Once the last monomer ( $N$ ) touches the wall of the capsid, the force inside grows rapidly with a saturating trend at high number of monomers. The inset c) of

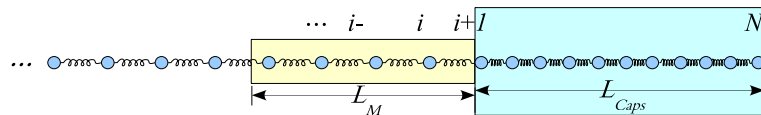


**Figure 7.** Scheme of the motor pushing the polymer inside the capsid of length  $L_{Caps}$ .

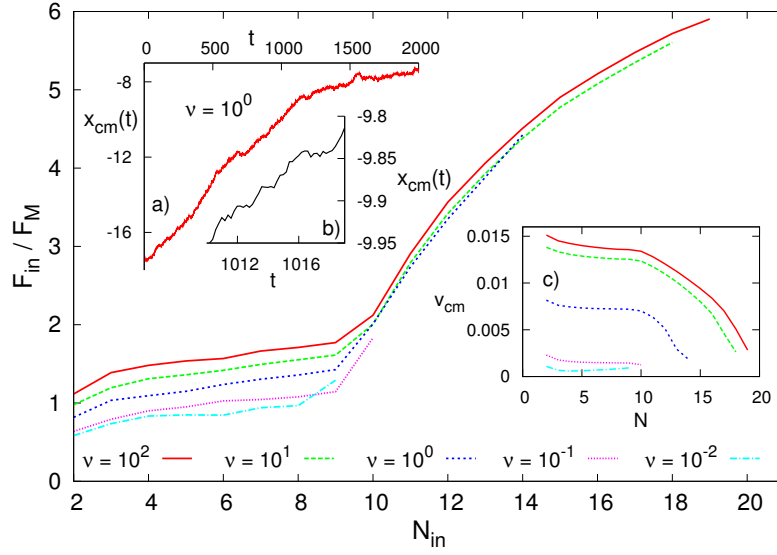


**Figure 8.** Force on the polymer as a function of the number of monomers entered inside the capsid ( $N_{in}$ ). This curve resembles the experimental outcome reported in [14]. The length of the capsid is  $L_{Caps} = 8$  and the number of monomer is  $N = 36$ . Insets: a) trajectory of the centre of mass  $x_{cm}$  with b) a small portion showing stops; c) chain velocity as a function of  $N_{in}$ . The activation rate of the motor for the calculations presented in the insets is  $\nu = 1$ .

the figure plots the polymer mean velocity  $vs$  the number of monomers in the capsid. We find a behaviour similar to that experimentally observed in [14]. It shows that the model here introduced can depict qualitatively the packing features of the  $\phi 29$  motor despite of its simplicity.

*Biological values.* The model we present here is a simplification of both a real polymeric chain and a molecular motor: in the example here used the DNA and the motor of the  $\phi 29$  bacteriophage.

The model is in principle adaptable to any translocation process mediated by ATP-based motors, provided that a proper scaling of the measurable quantities can be done. Experimental possible value of the working time of the motor is  $T_M = 10ms$ , of the affinity constant  $k_M \simeq 30\mu M$  [12], and of the saturation velocity  $v_{max} \simeq 103$  DNA base pairs/s =  $70nm/s$  [15]. The saturation velocity sets the  $v_{HR}$  value in our model, and the frequency at the Michaelis-Menten concentration corresponds to  $\nu = \nu_0 = 1/T_M$ . Finally, the stall force value found experimentally in the high frequency limit is  $F_{Stall}^{exp} = 57pN$  [14]. Using this value we can estimate  $F_M \approx 12pN$ . In the same way the energy consumed per cycle can be obtained for large ATP concentration as  $W = n_{mot}^{on} v_{max} F_M T_M$ . With the parameters used,  $W \approx 12kT_{room}$ , which is less than the energy provided by an ATP molecule, i.e. around  $20kT_{room}$ .

## 5. Discussion

In this work we have introduced a simple model for a molecular motor which consumes ATP and produces mechanical work pushing a polymer chain.

Other simple models have been used to describe translocation features of DNA. For instance, in the works by Downton a 1d polymer chain jointed together by a FENE potential is studied [18, 19]. The chain moves aided by a flashing extended ratchet potential. By contrast, our potential acts in a limited region of space which is a more realistic approach to translocation through a pore.

In our work, we calculate the mean translocation time and the velocity of the polymer as function of the activation frequency of the motor. The latter shows a very good agreement with the experiments and follows a clear Michaelis-Menten dependence with the ATP concentration. We see that such MM laws arise in a natural way in the description of the system as a consequence of the kinetics of a machine which remains active for a certain given time. It appears that the *working time average* of the molecular motors which use ATP, is actually the origin of the Michaelis-Menten law in ATP-motor assisted dynamics.

We have also studied the behaviour of the polymer in the presence of a pulling force and obtained analytical expressions for the stall force of the system as a function of the ATP concentration. Such expressions, a corrected MM equation, show an excellent agreement to our computed results. Finally, the force inside the capsid and the velocity of the chain as a function of the amount of polymer packed have been also evaluated finding good qualitative agreement with the experiments.

We have studied a one dimensional model. Polymer translocation experiments are usually performed with the help of optical traps. That way, the polymer (DNA or RNA) is held almost completely stretched out. With respect to the capsid effect, the confinement introduced in the model describes a saturating pressure inside the capsid without taking into account specific geometrical details and polymer recoil effects. For these two reasons the one-dimensional model is a good enough first approach to study the process.

Besides the fact that technological improvements allow nowadays very precise investigations at the nanoscale, the microscopic working details of the bacteriophage motors are not completely understood. The model is close to one of the two mechanisms recently proposed in [12], where the force acts by means of steric interactions, without chemical bonds with the DNA. Since DNA packing motor  $\phi 29$  is a well studied motor protein with several intriguing and unexplained features we have compared our results to experiments with this motor. In general we have found a good agreement. However, a detail model for  $\phi 29$  should include many other aspects and it is beyond the spirit and purpose of our work. Between these aspects we could mention a precise modelling of the inactive stage, the inclusion of more complex waiting time statistics or the addition of existing structural data.

The results here presented describe general features of a motor which actuates with

a mean force during its cycle. In this sense the qualitative results here reported need some adjustments of the parameters if applied in concrete cases and can be applied to a wide class of ATP-based motor, independently on the inner functioning of the very motor. Our work shows that our model could be a good starting point to develop detailed descriptions of different motors.

## Acknowledgments

This work was supported by Spanish MICINN through Project No.FIS2008-01240, cofinanced by FEDER funds.

## References

- [1] Zwolak M and di Ventra M 2008 *Rev. Mod. Phys.* **80** 141
- [2] Mickler M, Schleiff E and Hugel T 2008 *Chem. Phys. Chem.* **9** 1503
- [3] Kasianowicz J J, Brandin E, Branton D and Deamer D W 1996 *Proc. Natl. Acad. Sci. USA* **93** 13770
- [4] Schneider G F, Kowalczyk S W, Calado V E, Pandraud G, Zandbergen H W, Vandersypen L M K and Dekker C 2010 *Nano Lett.* **10** 3163
- [5] Metha D, Rief M, Spudich J A, Smith D A and Simmons R M 1999 *Science* **283** 1689
- [6] Starikov E B, Henning D, Yamada H, Gutierrez R, Norden B and Cuniberti G 2009 *Biophys. Rev. and Lett.* **4** 209
- [7] Gómez-Marín A and Sancho J M 2009 *Eur. Phys. Lett.* **86** 40002
- [8] Walter N G 2006 *Nat. Chem. Biol.* **2** 66
- [9] English B P, Min W, van Oijen A M, Lee K T, Luo G, Sun H, Cherayil B J, Kou S C and Xie X S 2006 *Nat. Chem. Biol.* **2** 87
- [10] Moffitt J R, Chemla Y R and Bustamante C 2010 *Proc. Natl. Acad. Sci.* **107** 15739
- [11] Rouse P E J 1953 *J. Chem. Phys.* **21** 1272
- [12] Moffitt J R, Chemla Y R, Aathavan K, Grimes S, Jardine P J, Anderson D L and Bustamante C 2009 *Nature* **457** 446
- [13] Pérez-Carrasco R and Sancho J M 2010 *Biophys. J.* **98** 2591
- [14] Smith D E, Tans S J, Smith S B, Grimes S, Anderson D L, and Bustamante C 2001 *Nature* **413** 748
- [15] Chemla Y R, Aathavan K, Michaelis J, Grimes S, Jardine P J, Anderson D L and Bustamante C 2005 *Cell* **122** 683
- [16] Fiasconaro A, Mazo J J and Falo F 2010 *Phys. Rev. E* **82** 031803
- [17] Fiasconaro A, Mazo J J and Falo F 2011 *J. Stat. Mech.* P11002
- [18] Downton M T, Zuckermann M J, Craig E M, Plischke M and Linke H 2006 *Phys. Rev. E* **73** 011909
- [19] Craig E M, Zuckermann M J and Linke H 2006 *Phys. Rev. E* **73** 051106